Proton Irradiations at Ultra-High Dose Rate vs. Conventional Dose Rate: Strong Impact on Hydrogen Peroxide Yield

Guillaume Blain, Johan Vandenborre, Daphnée Villoing, Vincent Fiegel, Giovanna Rosa Fois, Ferid Haddad, Charbel Koumeir, Lydia Maigne, Vincent Métivier, Freddy Poirier, et al.

Proton irradiations at ultra-high dose rate vs. conventional dose rate: Strong impact on hydrogen peroxide yield

Guillaume Blain[1], Johan Vandenborre[1], Daphnée Villoing[2], Vincent Fiegel[2], Giovanna Rosa Fois[3], Ferid Haddad[1,4], Charbel Koumeir[4], Lydia Maigne[3], Vincent Métivier[1], Freddy Poirier[4], Vincent Potiron[2], Stéphane Supiot[2], Noël Servagent[1], Grégory Delpon[2], Sophie Chiavassa[2]

[1] Laboratoire SUBATECH, UMR 6457, CNRS IN2P3, IMT Atlantique, Université de Nantes, France

[2] Institut de Cancérologie de l'Ouest, Saint-Herblain, France

[3] Université Clermont Auvergne, CNRS/IN2P3, LPC, 63000 Clermont-Ferrand, France

[4] GIP ARRONAX, Saint-Herblain, France

ABSTRACT:

Background: During ultra-high dose rate (UHDR) external radiation therapy, healthy tissues appear to be spared while tumor control remains the same compared to conventional dose rate. However, the understanding of radiochemical and biological mecanisms involved is still to be discussed.

Methods: This study shows how the hydrogen peroxide (H_2O_2) production, one of the Reactive Oxygen Species (ROS), could be controlled by early heterogenous radiolysis processes in water during UHDR proton beam irradiations. Pure water was irradiated in the plateau region (T.S. : track-segment) with 68 MeV protons under conventional (0.2 Gy/s) and several UHDR conditions (40 Gy/s to 60 kGy/s) at the Arronax cyclotron. Production of H_2O_2 was then monitored using the Ghormley triodide method.

Results: New values of $G_{TS}(H_2O_2)$ were added in conventional dose rate. A substantial decrease in H_2O_2 production was observed from 0.2 to 1.5 kGy/s with a more dramatic decrease below 100 Gy/s. At higher dose rate, up to 60 kGy/s, the H_2O_2 production stayed stable with a mean decrease of 38% ± 4%.

Conclusions: This finding, associated to the decrease in the production of hydroxyl radical (°OH) already observed in other studies in similar conditions can be explained by the well known spur theory in radiation chemistry. Thus, a two step FLASH-RT mechanism can be envisioned: an early step at the microsecond scale mainly controlled by heterogenous radiolysis, and a second, slower, dominated by O_2 depletion and biochemical processes. To validate this hypothesis, more measurements of radiolytic species will soon be performed, including radicals and associated lifetimes.

Background

Radiation therapy at ultra-high dose rate (UHDR, > 40 Gy/s), has recently shown promising benefits with a reduction in normal tissue toxicity while maintaining the tumor control. This observation, also called FLASH effect, was first shown with electron beams on mammalian cells *[1]* and more recently on various animal models: mice *[2-5]*, zebrafish embryos *[6, 7]*, cats and mini-pigs *[8]*. The first patient was treated in 2019 *[9]*. The FLASH effect was also demonstrated with X-Rays *[10, 11]*, protons *[12-15]* and helium ions *[16]*.

The mechanisms underlying the FLASH effect are still unclear and appear to be multiple and interrelated *[17, 18]*. A direct consequence of UHDR irradiations, compared to irradiations at conventional dose rate is a local higher concentration of free radicals within a short time interval, that may modify the chemical pathways. Numerous studies have shown the role of oxygen concentration in the FLASH effect *[6, 7, 19]* and this assumption was integrated in various models *[20-22]*. However, recent studies came to the conclusion that oxygen depletion and transient hypoxia might not be the main mechanism of the FLASH effect *[23-25]*. Among the other explored mechanisms, the impact on radical production and recombination could have an important role in the FLASH effect *[7, 10, 17, 25]*. To corroborate the hypothesis that ultra-high and conventional dose rates do not produce the same levels of specific radicals, Montay-Gruel et al. *[6]* compared Hydrogen Peroxide (H_2O_2) produced after UHDR and conventional dose rate irradiations for electron beams (6 MeV) in water. They measured a significant decrease of H_2O_2 after UHDR (~ 500 Gy/s) compared to conventional dose rate (~ 0.3 Gy/s). Similarly, Kusumoto et al. *[26]* evaluated radiolytic yield (G values) of 7-hydroxy-coumarin-3-carboxylic acid (7OH-C3C4) as a radical scavenger of hydroxyl radicals (°OH) while varying the mean dose rate of proton beam (27.5 MeV) from 0.05 to 160 Gy/s. The G value of produced 7OH-C3C4, which is strongly associated to °OH, decreases with an increasing dose rate.

This study aims to investigate the decrease in the production of H_2O_2 in UHDR irradiations conditions with proton beams. Moreover, we studied the variation of track-segment H_2O_2 production yield with the mean dose rate for 10 dose rates between 0.2 Gy/s to 60 kGy/s.

Materials and Methods

ARRONAX facilities and experimental setup

ARRONAX is an isochronous cyclotron (IBA Cyclone 70XP) that produces protons from 30 MeV up to 70 MeV, deuterons from 15 MeV up to 35 MeV and alpha particles at a fixed energy of 68 MeV. It offers the possibility of delivering protons beams at dose rates ranging from conventional dose rate to UHDR thanks to available beam intensities (proton intensity can vary from 1 pA to 350 µA) and a homemade pulsing device developed and validated in house *[27]*. This system allows from bunches of protons interspaced by 32.84 ns (micro-pulse, RF = 30.45 MHz) to adjust the duration of the irradiation (>10 µs) and the frequency rate of the macro-pulse repetition, allowing an easy shift between conventional dose rate and UHDR irradiations and a flexible beam structure.

Experimental setups

Our experimental setups for H_2O_2 measurements with 68 MeV proton beams were directly adapted from our irradiation setups designed for the irradiation of zebrafish embryos (Figure 1). A first setup (#1), with a large source-target distance (Figure 1A) enabled a maximal pulse dose rate of 7.5 kGy/s. A second setup (#2) with a shorter source-target distance (Figure 1B) allowed to increase the pulse dose rate up to 60 kGy/s. On Figure 1, K corresponds to a kapton beam exit window, TF to a 50µm tungsten foil and C1 (Ø 15 mm) and C2 (Ø 10 mm) to aluminum collimators. This set of elements were used to spread and homogenize the beam. An online dosimetry was performed with a R928 Hamamatsu Photonics photomultiplier tube (PMT) measuring the UV photons emitted from excited nitrogen of the air present on the path of the incident beam *[28]*, together with an in-transmission parallel-plate ionization chamber (IC) (model 34058, PTW, Freiburg, Germany). Both detectors were calibrated at the beginning of each experiment using a Faraday cup (FC) with an electron repeller positionned after the target, and connected to a MULTIDOS high-precision electrometer (PTW Freiburg GmbH). A dose uncertainty of 1.5% was assessed in conventional dose rate with the IC, whereas a 3% dose uncertaintywas estimated in UHDR conditions using the PMT.

A rack was designed and 3D-printed to support twelve 1.5 mL Eppendorf tubes. Each Eppendorf tube was filled with 1.4 mL of ultrapure purewater(ρ=18.2MΩ.cm), closed under air condition and placed far enough from the other tubes (6 cm center to center) to avoid the impact of scattered radiations from one tube to the other (Figure 2A). The beam was directed to the cylindrical part of each tube and laterally centered (Figure 2B). Sample tubes received a track-segment irradiation, while Bragg peak was deposited inside the faraday cup (FC). The average L.E.T. is calculated at 1.17keV.µm-1 ±6.5% using a monte-carlo calculation *[29]* . The rack was placed on an in-house automatic XY translator built using two high-precision linear stages with step motor.

Beam structures

With these experimental setups and a single pulse, the maximal mean dose rate achieved in Eppendorf tubes was around 7.5 kGy/s for setup #1 and 60 kGy/s for setup #2. Using the minimal intensity, the corresponding minimal pulse dose rates were 2.5 Gy/s and 40 Gy/s for setup #1 and #2 respectively. To set a conventional dose rate around 0.2 Gy/s (12 Gy/min), multiple pulses were used and both intensity and frequency were adjusted (Table 1). With setup #1, five UHDR proton irradiations were performed considering a single pulse and mean dose rates from 50 Gy/s to 7.5 kGy/s. While with the setup #2, four UHDR proton irradiations were performed using a single pulse and mean dose rates from 40 Gy/s to 60 kGy/s.

H_2O_2 measurements

Concentrations of H_2O_2 have been determined post-irradiation (about 15 min after irradiation), using the Ghormley triiodide method *[30]* and two reagents. One is a mixture of ammonium molybdate ($Mo_7O_{24}(NH_4)$ $2H_2O$), potassium iodide (KI) and sodium hydroxide (NaOH) and the second one is a buffer solution (pH 4–5) of acid potassium phthalate ($C_8H_5KO_4$). For a total volume of 2.8 mL, 0.7 mL of both reagents were mixed with 1.4 mL of the sample solution. The concentration of H_2O_2 was obtained indirectly by measurement of I_3^- absorbance using a CARY4000 (VARIAN) spectrophotometer. The molar extinction coefficient of I_3^- at 351 nm wavelength was previously determined at 21260 $L.mol^{-1}$ $.cm^{-1}$ in the studied solution at 298 K.

Radiolytic yield calculation

The radiolytic yield (G) is defined as the number of species formed or consumed per unit of deposited energy. It is expressed in the international system in $mol.J^{-1}$ and is calculated at a time *t* after transition of the ionizing irradiation according to:

$$G(X) = \frac{X_t}{\rho\, D} \qquad (1)$$

where X_t is the concentration of the species X at time *t* ($mol.L^{-1}$), ρ is the volumic mass of the irradiated solution ($kg.L^{-1}$) and D the absorbed dose (in Gy; 1 Gy = 1 $J.kg^{-1}$ of water).

Results

We observed a significantly lower concentration of H_2O_2 for all doses above 10 Gy in UHDR proton irradiations compared to conventional ones with setup #1 (Figure 3) and setup #2 (Figure 4). These measurements were repeated on independent experiments (2 or 3 times). Track segment $G_{TS}(H_2O_2)$ values were extracted from the linear fit of these measurements and mean values from repeated measurements are shown in Figure 5 and Table 2.

At a conventional dose rate, we obtained a new $G_{TS}(H_2O_2)$ equal to $0.98 \pm 0.05\ 10^{-7}$ mol J^{-1} (Table 2). As proton dose rate increases, $G_{TS}(H_2O_2)$ decreases as function of dose rate up to 1.5kGy/s and then remains constant above 7.5 kGy/s with a mean decrease of 38% ± 4% (Figure 5 and Table 2). Decrease is already seen at 40Gy/s (-23%).

Discussion

Our experiments with proton beams confirmed the results of lower H_2O_2 production yields in UHDR irradiation compared to conventional dose rate irradiation obtained with electron beams by Montay-Gruel et al *[6]*. We found a slightly higher decrease in H_2O_2 production yields in the present study. This finding supports the hypothesis that UHDR irradiations have an impact on the ROS production.

This is particularly interesting when considering the major differences between the beams of these two studies, besides the particle type. The conventional mean dose rate used by Montay-Gruel *et al. [6]* (0.29 Gy/s) was quite similar to our conventional dose rate of 0.20 Gy/s. The mean dose rate in UHDR conditions applied by Montay-Gruel *et al. [6]* was around 500 Gy/s, which was reproduced in our experiment. However, beam structures were very different in the two studies. For UHDR irradiations, Montay-Gruel *et al. [6]* used multiple very short pulses (pulse width < 2 μs) while we applied longer single pulses, in the millisecond range. Electrons intra-pulse dose rates from Montay-Gruel *et al. [6]* were much higher than ours in UHDR conditions ($2.8\ 10^6$ Gy/s vs. 40 Gy/s to 60 kGy/s) as well as for conventional dose rates ($2.8\ 10^4$ Gy/s vs. 2.5 and 40 Gy/s, depending on the setup used in our experiments).

In this study, we investigated the variation of $G_{TS}(H_2O_2)$ for a large range of mean dose rates in UHDR conditions, from the minimal dose rate of 40 Gy/s ever considered for FLASH radiotherapy in the literature *[31]*. We find a decrease of $G_{TS}(H_2O_2)$ with an increasing dose rate up to 1.5 kGy/s, with a more dramatic decrease below 100 Gy/s, and followed by a plateau (38% ±4%) up to 60 kGy/s. In the study of Kusumoto *et al. [26]*, on 7OH-C3C4 giving information on °OH production, they used three low mean dose rates (0.05, 0.8 and 7.7 Gy/s) and two UHDR (80 and 160 Gy/s). The G value of produced 7OH-C3C4 decreased steadily with an increasing dose rate and tended to saturate above 80 Gy/s. These findings are in line with our results concerning H_2O_2 and give some hints on the ROS production landscape with a reduced production of OH° and H_2O_2 in proton conditions that reached a plateau above 160 Gy/s in both cases. These behaviours could be explained considering the long-established water radiolysis reactions *[32]*. A lack of °OH, and therefore a lack of H_2O_2 which is produced throught the °OH - °OH reaction (Eq.1), could be explained by a faster reaction of °OH with aqueous electron radicals (e^-_{aq}) (Eq.2) inside the spurs and overlapping spurs, created by the interaction of the incident particle with water. With this spur theory, we suggest that UHDR conditions would favor the °OH - e^-_{aq} reaction (Eq.2) vs.the °OH - °OH one (Eq.1), due to a higher reaction kinetic rate and the high density of radiolytic species created in these conditions:

$°OH + °OH \rightarrow H_2O_2$ ($2k = 1.1\ 10^{10}\ M^{-1}.s^{-1}$) Eq.1

$°OH + e^-_{aq} \rightarrow OH^-$ ($k = 3.00\ 10^{10}\ M^{-1}.s^{-1}$) Eq.2

Indeed, in UHDR conditions, there is an increased local dose deposition in time and space coming from the short duration of the irradiation that leads to increased local radical concentrations and that would emphasize this phenomenon. Remaining radicals could then diffuse in medium leading to conditions that are close to that obtained in conventional dose rate irradiations outside spurs (homogeneous chemistry step) and process as usual to recombinations with the medium. However, even with higher constant rates in Eq.2, all °OH radicals will not be scavenged, which could explain why H_2O_2 production is never completely avoided, even at 60 kGy/s in the present study. Further experiments will be performed to scavenge aqueous electrons and measure the impact on H_2O_2 production in order to test this hypothesis. In addition, H_2O_2 measurements for intermediate mean dose rates between 0.2 and 40 Gy/s will be studied to allow more comparison with Kusumoto et al.*[26]*.

Conclusions

In this work, impact of protons at ultra-high dose rates on the hydrogen peroxide concentration was studied for a wide range of dose rates (from 40 Gy/s up to 60 kGy/s). A decrease in H_2O_2 production yields (38% ±4%) was observed in UHDR conditions compared with conventional ones, which seems to be induced by chemical reactions between several radiolytic species such as e^-_{aq}, °OH and H°. In particular, two steps mechanisms might be involved in the mecanism: (1) a faster one (under the µs scale) with reactions between highly localy concentrated radicals (e^-_{aq}, °OH and H°) in spurs that lead to produce less ROS, (2) a slower one (at the ms scale) which involves radiolytic molecules (H_2O_2, H_2), remaining radicals and oxygen present in biological tissues. Therefore, in order to understand the mechanisms underlying the FLASH effect, the radiolytic mechanisms should first be investigated extensively. Experimental data should be used as input for models that intend to simulate the production and diffusion of ROS after irradiation under UHDR conditions. Our next efforts will focus on the determination of $G(e^-_{aq})$ in conventional and UHDR conditions and its comparison with the G of other radicals such as °OH and H°.

Acknowledgment

This work has been supported in part by a grant from the French National Agency for Research called "Investissements d'Avenir", Equipex ArronaxPlus n°ANR-11-EQPX-0004, Labex IRON (ANR-11-LABX-18-01) and ISITE NExT n°ANR-16-IDEX-0007. The authors would like to express their gratitude to ARRONAX facility teams for their technical support in this study, and Rudi Labarbe and his colleagues for helpful scientific discussions.

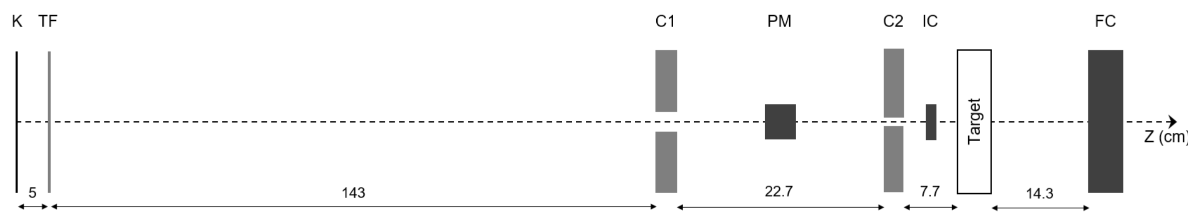

Setup #1

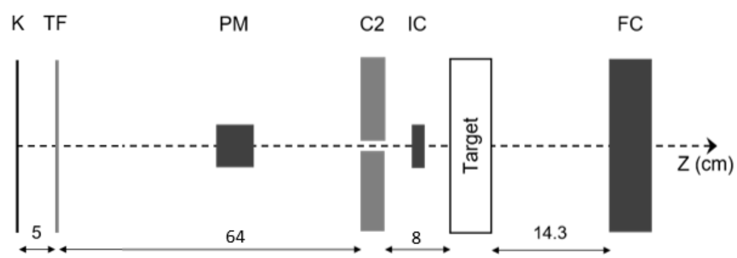

Setup #2

Figure 1. Proton beam experimental setup #1 with a large distance allowing a maximal pulse dose rate about 7.5 kGy/s and experimental setup #2 with a shorter distance allowing a maximal pulse dose rate about 60 kGy/s. K = Kapton (beam exit window); TF = Tungsten foil; C1 = 1^{st} collimator Ø 15 mm; PM = Photomultiplier tube; C2 = 2^{nd} collimator Ø 10 mm; IC = ionization chamber; FC = Faraday cup Ø 30 mm.

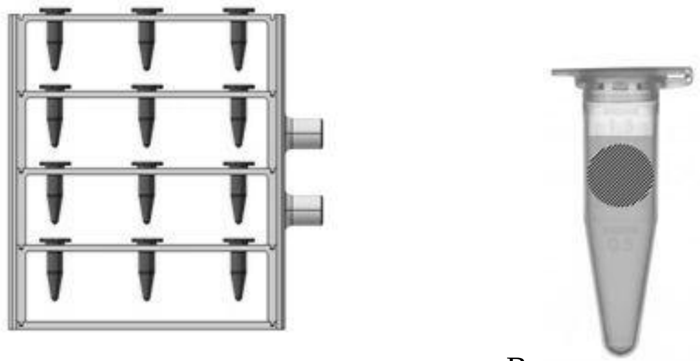

A. B.

Figure 2. (A) 3D-printed Eppendorf tubes rack to be fixed on the in-house automatic XY translator. (B) 1cm diameter beam presented on a 1.5 mL Eppendof tube, filled with 1.4 mL of water.

Table 1: Beam structures to deliver 6 doses values in conventional and UHDR irradiation modes for setup #1 and #2.

Setup	Mean dose rate (Gy/s)	Pulse Dose rate (Gy/s)	Number of pulses	Pulse width (ms)	Frequency (Hz)	Doses (Gy)
Setup #1	0.2	2.5	[2400 – 40500]	0.80	100	[5, 10, 20, 30, 40, 80]
	$7.5\ 10^3$	$7.5\ 10^3$	1	[0.67 – 10.67]	-	
	$1.5\ 10^3$	$1.5\ 10^3$		[3.30 – 53.30]		
	500	500		[10.0 – 160.0]		
	100	100		[50.0 – 800.0]		
	50	50		[100.0 – 1600.0]		
Setup #2	0.20	40	[1500 – 20550]	0.10	50	[10, 20, 30, 40, 60, 80]
	$60\ 10^3$	$60\ 10^3$	1	[0.167 – 1.33]	-	
	$40\ 10^3$	$40\ 10^3$		[0.25 – 2.0]		
	$20\ 10^3$	$20\ 10^3$		[0.50 – 4.0]		
	40	40		[250.0 – 2000.0]		

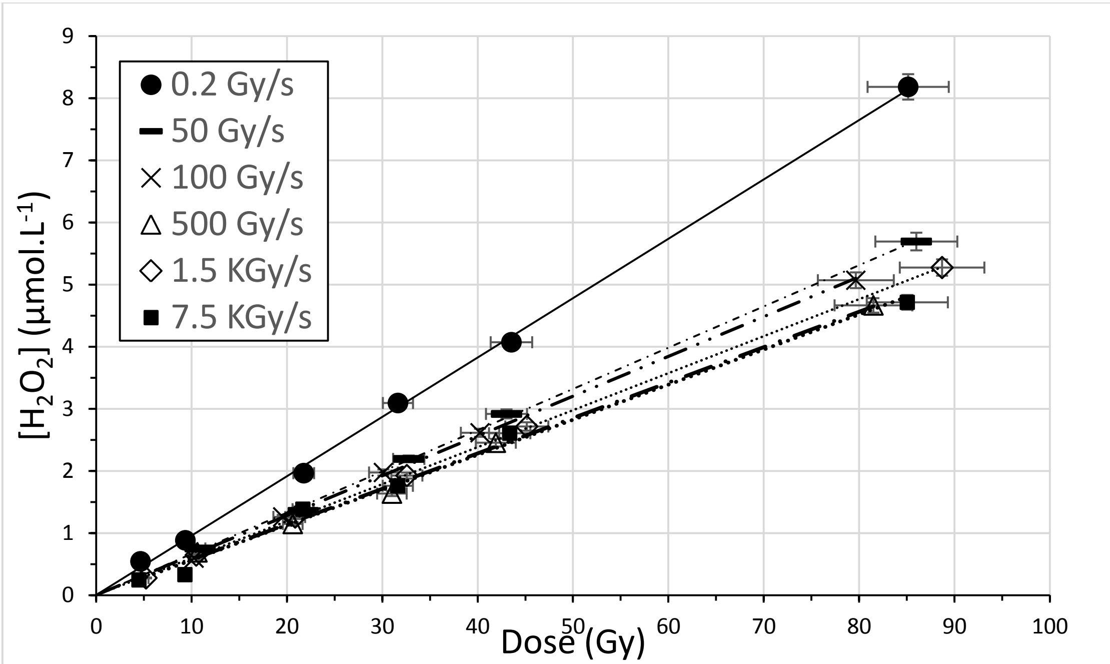

Figure 3: H_2O_2 measurement with the setup #1: five ultra high dose rates from 50Gy/s to 7.5 kGy/s with the same beam structure (single pulse), and one conventional dose rate of 0.2 Gy/s (multiple pulses). For the sake of readability, only one dataset per dose rate is shown among all measured data.

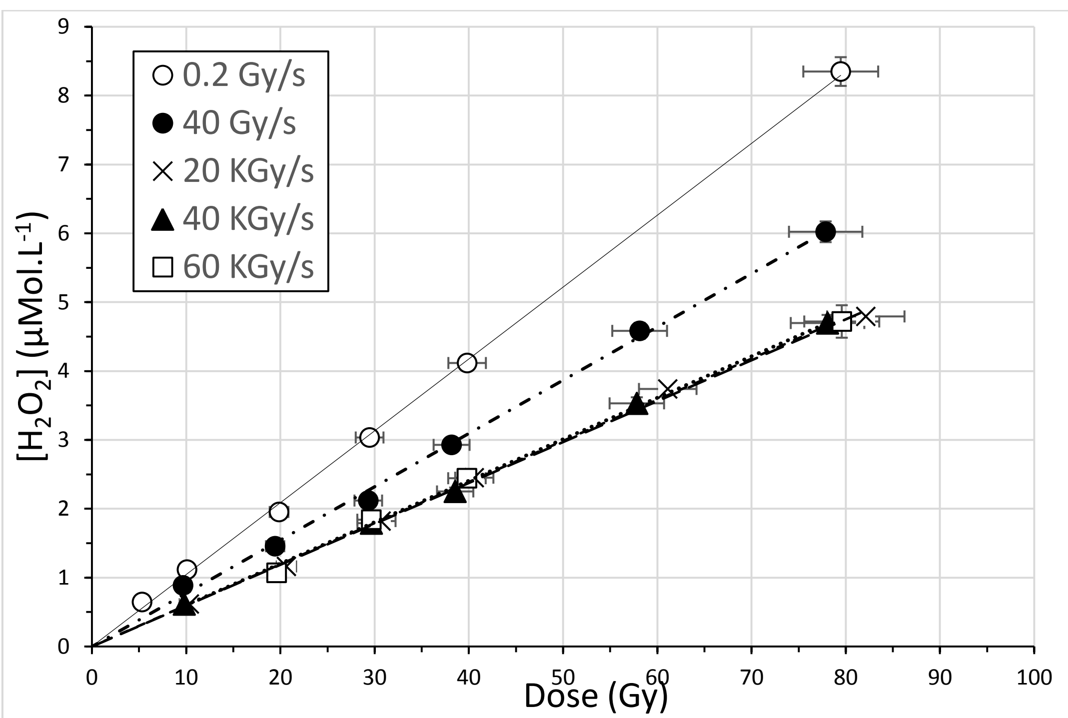

Figure 4: H_2O_2 measurement with the setup #2: four UHDR from 40Gy/s to 60 kGy/s with the same beam structure (single pulse) and one conventional dose rate of 0.2 Gy/s (multiple pulses). For the sake of readability, only one dataset per dose rate is shown among all measured data.

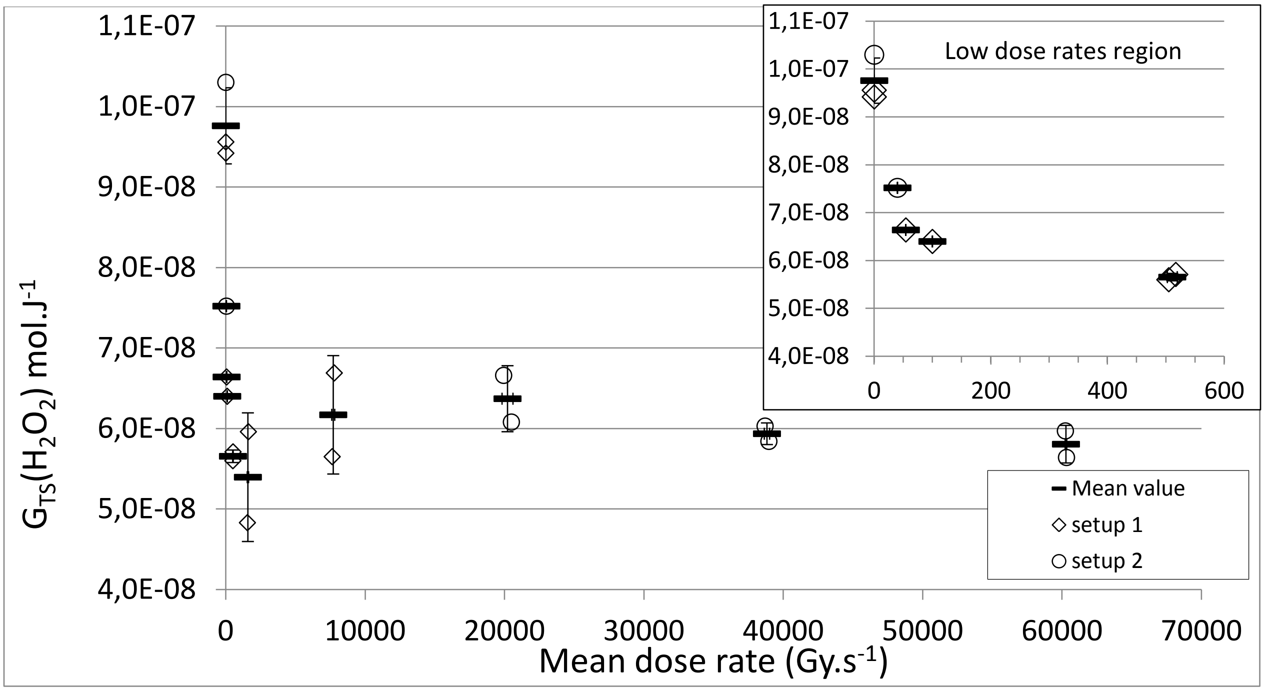

Figure 5: $G_{TS}(H_2O_2)$ in mol.J^{-1} for all experiments (setup #1 and #2).

Table 2: $G_{TS}(H_2O_2)$ obtained for conventional and UHDR irradiations. G values are obtained from experiments presented on Figures 3 and 4 for setup #1 and #2 for six different doses and a linear trend line.

Mean dose rate (Gy/s)	$G_{TS}(H_2O_2)$ 10^{-7} mol/J	Mean $G_{TS}(H_2O_2)$ 10^{-7}mol/J (SD)	R^2	Decrease (%) in UHDR $G(H_2O_2)$ from mean conventional $G_{TS}(H_2O_2)$
0.20	0.96 1.03 0.94	0.98 (4.7e-3)	0.999 0.999 0.997	-
40	0.75	-	0.997	23
50	0.66	-	0.999	32
100	0.64	-	0.999	34
500	0.56 0.57	0.57 (7.8e-4)	0.997 0.997	43 41
$1.5\ 10^3$	0.48 0.60	0.54 (8.0e-3)	0.996 1.000	51 39

7.5 10^3	0.57 0.67	0.62 (7.4e-3)	0.993 0.994	42 31
20 10^3	0.67 0.61	0.64 (4.1e-3)	0.990 0.999	32 38
40 10^3	0.58 0.60	0.59 (1.3e-3)	0.999 0.999	40 38
60 10^3	0.60 0.56	0.58 (2.3e-3)	0.997 0.986	39 42

References

[1] Town CD. Effect of High Dose Rates on Survival of Mammalian Cells. Nature 215:847-8, 1967.

[2] Favaudon V, Caplier L, Monceau V, Pouzoulet F, Sayarath M, Fouillade C, Poupon MF, Brito I, Hupé P, Bourhis J, Hall J, Fontaine JJ and Vozenin MC. Ultrahigh dose-rate FLASH irradiation increases the differential response between normal and tumor tissue in mice. Science translational medicine 6, 245, 2014.

[3] Fouillade C, Curras-Alonso S, Giuranno L, Quelennec E, Heinrich S, Bonnet-Boissinot S, Beddok A, Leboucher S, Karakurt HU, Bohec M, Baulande S, Vooijs M, Verelle P, Dutreix M, Londono-Vallejo JA and Favaudon V. FLASH irradiation spares lung progenitor cells and limits the incidence of radio-induced senescence. Clinical Cancer Research 26: 1497-1506, 2020.

[4] Levy K, Natarajan S, Wang J, Chow S, Eggold JT, Loo PE, Manjappa R, Melemenidis S, Lartey FM, Schüler E, Skinner L, Rafat M, Ko R, Kim A, Al-Rawi DH, von Eyben R, Dorigo O, Casey KM, Graves EE, Bush K, Yu AS, Koong AC, Maxim PG, Loo BW and Rankin EB. Abdominal FLASH irradiation reduces radiation-induced gastrointestinal toxicity for the treatment of ovarian cancer in mice. Scientific Reports 10:21600, 2020.

[5] Montay-Gruel P, Petersson K, Jaccard M, Boivin G, Germond JF, Petit B, Doenlen R, Favaudon V, Bochud F, Bailat C, Bourhis J and Vozenin MC. Irradiation in a flash: Unique sparing of memory in mice after whole brain irradiation with dose rates above 100Gy/s. Radiotherapy and Oncology 124:365-69, 2017.

[6] Montay-Gruel P, Acharya MM, Petersson K, Alikhani L, Yakkala C, Allen BD, Ollivier J, Petit B, Jorge PG, Syage AR, Nguyen TA, Baddour AAD, Lu C, Singh P, Moeckli R, Bochud F, Germond JF, Froidevaux P, Bailat C, Bourhis J, Vozenin MC and Limoli CL. Long-term neurocognitive benefits of FLASH radiotherapy driven by reduced reactive oxygen species. Proceedings of the National Academy of Sciences 116:10943-51, 2019

[7] Vozenin MC, Hendry JH and Limoli CL. Biological Benefits of Ultra-high Dose Rate FLASH Radiotherapy: Sleeping Beauty Awoken. Clinical Oncology 31:407-15, 2019.

[8] Vozenin MC, De Fornel P, Petersson K, Favaudon V, Jaccard M, Germond JF, Petit B, Burki M, Ferrand G, Patin D, Bouchaab H, Ozsahin M, Bochud F, Bailat C, Devauchelle P and Bourhis J. The advantage of FLASH radiotherapy confirmed in mini-pig and cat-cancer patients. Clinical Cancer Research 25:35-42, 2019.

[9] Bourhis J, Sozzi WJ, Jorge PG, Gaide O, Bailat C, Duclos F, Patin D, Ozsahin M, Bochud F, Germond JF, Moeckli R and Vozenin MC. Treatment of a first patient with FLASH-radiotherapy. Radiotherapy and Oncology 139:18-22, 2019.

[10] Berry RJ, Hall EJ, Forster DW, Storr TH and Goodman MJ. Survival of mammalian cells exposed to x rays at ultra-high dose-rates. The British journal of radiology 42:102-107, 1969.

[11] Montay-Gruel P, Bouchet A, Jaccard M, Patin D, Serduc R, Aim W, Petersson K, Petit B, Bailat C and Bourhis J. X-rays can trigger the FLASH effect: Ultra-high dose-rate synchrotron light source prevents normal brain injury after whole brain irradiation in mice. Radiotherapy and Oncology 129:582-88, 2018

[12] Buonanno M, Grilj V and Brenner DJ. Biological effects in normal cells exposed to FLASH dose rate protons. Radiotherapy and Oncology 139:51-55, 2019.

[13] Cunningham S, McCauley S, Vairamani K, Speth J, Girdhani S, Abel E, Sharma RA, Perentesis JP, Wells SI, Mascia A and Sertorio M. FLASH Proton Pencil Beam Scanning Irradiation Minimizes Radiation-Induced Leg Contracture and Skin Toxicity in Mice. Cancers 13, 1012, 2021.

[14] Diffenderfer ES, Verginadis II, Kim MM, Shoniyozov K, Velalopoulou A, Goia D, Putt M, Hagan S, Avery S and Teo K. Design, implementation, and in vivo validation of a novel proton FLASH radiation therapy system. Int. J. of Radiat. Oncol. Biol. Phys 106:440-448, 2020

[15] Zhang Q, Cascio E, Li C, Yang Q, Gerweck LE, Huang P, Gottschalk B, Flanz J and Schuemann J. Flash investigations using protons: Design of delivery system, preclinical setup and confirmation of flash effect with protons in animal systems. Radiation Research 194:656-64, 2020.

[16] Tessonnier T, Mein S, Walsh DW, Schuhmacher N, Liew H, Cee R, Galonska M, Scheloske S, Schömers C, Weber U. FLASH dose-rate helium ion beams: first in vitro investigations. Int. J. of Radiat. Oncol. Biol. Phys, 111(4):1011-22, 2021

[17] Wardman P. Radiotherapy Using High-Intensity Pulsed Radiation Beams (FLASH): A Radiation-Chemical Perspective. Radiation Research 194:607-17, 2020.

[18] Zhou, G. Mechanisms underlying FLASH radiotherapy, a novel way to enlarge the differential responses to ionizing radiation between normal and tumor tissues. Radiation Medicine and Protection 1:35-40, 2020

[19] Adrian G, Konradsson E, Lempart M, Bäck S, Ceberg C and Petersson K. The FLASH effect depends on oxygen concentration. The British journal of radiology 92, 20190702, 2020.

[20] Petersson K, Adrian G, Butterworth K and McMahon SJ. A quantitative analysis of the role of oxygen tension in FLASH radiation therapy. Int. J. of Radiat. Oncol. Biol. Phys 107:539-47, 2020.

[21] Pratx G and Kapp DS. A computational model of radiolytic oxygen depletion during FLASH irradiation and its effect on the oxygen enhancement ratio. Physics in Medicine & Biology 64: 185005, 2019.

[22] Spitz DR, Buettner GR, Petronek MS, St-Aubin JJ, Flynn RT, Waldron TJ and Limoli CL. An integrated physico-chemical approach for explaining the differential impact of FLASH versus conventional dose rate irradiation on cancer and normal tissue responses. Radiotherapy and Oncology, 139:23-7, 2019.

[23] Boscolo D, Scifoni E, Durante M, Krämer M and Fuss M.C. May Oxygen depletion explain the FLASH effect? A chemical track structure analysis. Radiotherapy and Oncology, 162:68-75, 2021.

[24] Cao X, Zhang R, Esipova TV, Allu SR, Ashraf R, Rahman M, Gunn JR, Bruza P, Gladstone DJ, and Williams BB, 2021. Quantification of Oxygen Depletion During FLASH Irradiation In Vitro and In Vivo. Int. J. of Radiat. Oncol. Biol. Phys. 111:241-8, 2021.

[25] Labarbe R, Hotoiu L, Barbier J and Favaudon V. A physicochemical model of reaction kinetics supports peroxyl radical recombination as the main de terminant of the Flash effect. Radiotherapy and Oncology 153:303-10, 2020.

[26] Kusumoto T, Kitamura H, Hojo S, Konishi T and Kodaira S. Significant changes in yields of 7-hydroxy-coumarin-3-carboxylic acid produced under FLASH radiotherapy conditions. RSC Advances 10:38709-14, 2020.

[27] Poirier F, Blain G, Bulteau-harel F, Fattahi M, Goiziou X, Haddad F, Koumeir C, Letaeron A and Vandenborre J. The Pulsing Chopper-Based System of the Arronax C70XP Cyclotron. International Partile Accelerator Conference, 1948-50, 2019.

[28] Lill J-O. Charge integration in external-beam PIXE. Nucl Instrum Methods Phys Res Sect B Beam Interact Mater At. 150(1):114-117, 1999.

[29] Sarrut D, Bardiès M, Boussion N, et al. A review of the use and potential of the GATE Monte Carlo simulation code for radiation therapy and dosimetry applications. Med Phys. 2014;41(6):064301.

[30] Ghormley JA and Hochanadel CJ. The Yields of Hydrogen and Hydrogen Peroxide in the Irradiation of Oxygen saturated Water with Cobalt γ-Rays. J. Am. Chem. Soc. 76:3351-52, 1954.

[31] Bourhis J, Montay-Gruel P, Goncalves Jorge P, Bailat C, Petit B, Ollivier J, Jeanneret-Sozzi W, Ozsahin M, Bochud F, Moeckli R, Germond JF and Vozenin MC. Clinical translation of FLASH radiotherapy: Why and how ? Radiotherapy and Oncology 139:11-7, 2019.

[32] Allen AO. The Radiation Chemistry of Water and Aqueous Solutions, Princeton, USA, 1961.